

Development And Application Of A Negative Stiffness Device

Jianxiu Xu¹, Xiaosheng Song²

¹North China University of Technology, Tangshan 063021, China;

²North China University of Technology, Tangshan 063021, China.

Abstract

In order to effectively reduce the seismic response, it is usually necessary to arrange a certain number of energy dissipating and damping devices between floors. If the single energy dissipating damping device is arranged less, it is difficult to achieve the expected effect, and too much arrangement will increase the rigidity of the building structure. , To a certain extent, increase the seismic response. Therefore, the combined arrangement of the negative stiffness structure and the energy dissipation device can effectively solve the above problems.

Keywords

Damping response; negative stiffness; framework.

1. Introduction

In order to effectively reduce the seismic response, it is usually necessary to arrange a certain number of energy dissipating and damping devices between floors. If the energy dissipating and damping devices are arranged less, it is difficult to achieve the expected effect, and too much arrangement will increase the rigidity of the building structure. , To a certain extent, increase the seismic response. Therefore, the combined arrangement of the negative stiffness structure and the energy dissipation device can effectively solve the above problems.

Japanese scholar Lemura introduced the concept of negative stiffness into the field of structural control, using negative stiffness devices to offset the increased stiffness of the damper, which can achieve a good control effect that not only reduces the structural shear but also limits the displacement [1]. Contrary to the positive stiffness, the negative stiffness does not hinder the deformation of the structure, but reduces the resistance to the deformation of the structure and promotes the deformation of the structure. The negative stiffness device itself is unstable, it has no load-bearing capacity, and large deformation will occur under any small load.

For this reason, Trimboli and Platus combined a positive stiffness spring and a negative stiffness spring, and proposed a mechanical isolation mechanism with positive stiffness springs in parallel, which improved the instability of the negative stiffness device [2, 3]. Subsequent scholar Lemura proposed a negative stiffness damper, which is connected in parallel with ordinary rubber isolation bearings, and this combination has a significant effect on reducing high-frequency seismic response [4]. Sun Tong et al. studied a new type of track-type negative stiffness device, which is composed of track blocks and spring-driven rollers [5]. It is proved that the negative stiffness device can significantly isolate the vibration, and it is also proved that the NSD control system has a better effect on the displacement control effect than the LQR semi-active control.

This paper proposes a negative stiffness device based on pre-compressed springs, and conducts theoretical derivation. Based on etabs analysis of the combined arrangement of negative stiffness and buckling braces, the effect of damping concrete frame structures under different seismic waves is analyzed, and its practical application possibilities are analyzed.

2. Design and Analysis of Negative Stiffness Device

2.1. Negative Stiffness Device Structure and Theoretical Derivation

2.1.1. Structure of negative stiffness device

The negative stiffness device shown in Figure 1 is composed of eight sets of pre-compression springs, four pairs of circular hinges and upper and lower vertical frames. The arrangement of the device in the building is similar to the arrangement of the damping wall, and the whole arrangement is between the floors, in which the upper frame is connected with the upper beam, and the lower frame is connected with the lower beam. The height of the device depends on the height between the building floors, and the width is the width of the fixed beam. When the structure is horizontally displaced under the action of an earthquake load, the upper and lower frames of the negative stiffness device are displaced to each other, generating a force that promotes the direction of the building's displacement and providing negative stiffness.

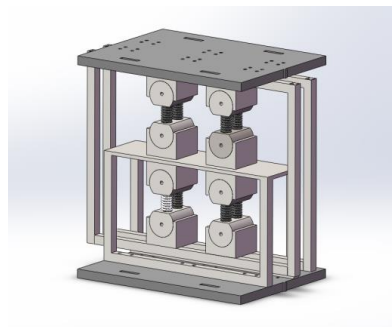
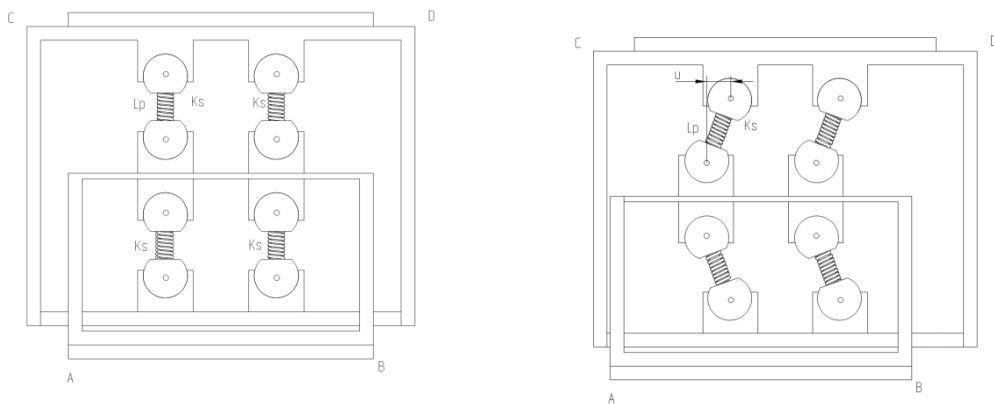


Fig. 1 Negative stiffness device model

2.1.2. Theoretical Derivation of Negative Stiffness Device

The basic schematic diagram of the negative stiffness device is shown in the figure, among them: the pre-compression spring provides initial pre-compression P_{in} when it is not deformed. When the upper frame CD and the lower frame AB of the device move relatively horizontally, and the displacement is u , the pre-compression spring deviates from the initial position. The pre-pressure produces a component along the direction of movement. When the middle plate is horizontally displaced to the maximum position, it begins to return to the initial position. The pre-pressure has a component that hinders the direction of movement, achieving a negative stiffness output.



(a) Undeformed negative stiffness device

(b) Deformation negative stiffness device

Fig. 2 Plan view of negative stiffness device

In order to simplify the analysis process of the negative stiffness device, the following assumptions are made:

All components are rigid and do not deform;

Ignore the weight of the device itself;

Ignore the influence of friction between round hinges;

Assuming that the horizontal displacement of the outer frame is u , the force F_s in the pre-compression spring changes with the movement of the device, and its value is:

$$F_s = P_{in} - K_s(l_s - l_p) \tag{1}$$

Where: the preload of the P_{in} preloaded spring, the stiffness of the main spring of K_s , the spring length of the l_s negative stiffness device when the movement displacement is u , and the length of the preloaded spring when the l_p negative stiffness device is not deformed.

Therefore, the horizontal force and displacement curve of the structure is:

$$F_{NSD} = \frac{F_s}{l_s} u = K_s \left(1 - \frac{l}{\sqrt{l^2(\lambda-1)^2 + u^2}} \right) u \tag{2}$$

$$K_{NSD} = K_s \left(1 + \frac{l u^2}{[l^2(\lambda+1)^2 + u^2]^{1.5}} \right) - \frac{l}{\sqrt{l^2(\lambda+1)^2 + u^2}} \tag{3}$$

$$l = \frac{l_p}{(1-\lambda)} \tag{4}$$

Where: λ spring compression ratio.

Table 1 gives the specific values of the parameters in the formula, and uses these values to calculate, the results are shown in Figure 3:

- (a) is the force-displacement relationship of the negative stiffness device based on formula (2);
- (b) is the stiffness change curve based on formula (3).

Table 1 Component parameters of negative stiffness device

| Name | Numerical value | Unit |
|---------------------------|-----------------|------|
| Spring length free length | 200 | mm |
| Preload spring stiffness | 88 | N/mm |
| Spring compression ratio | 0.2 | |
| Spring outer diameter | 60 | mm |
| Spring wire diameter | 10 | mm |

- (a) is the force-displacement relationship of the negative stiffness device based on formula (2);
- (b) is the stiffness change curve based on formula (3).

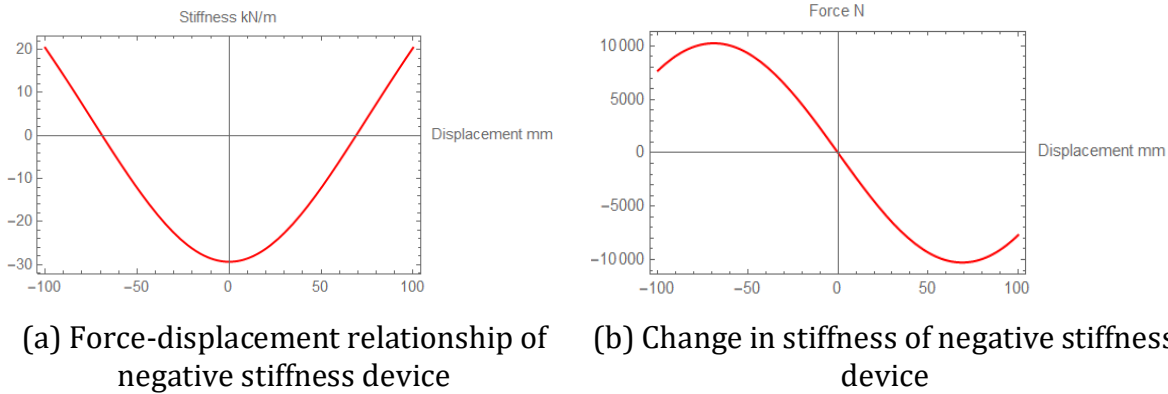
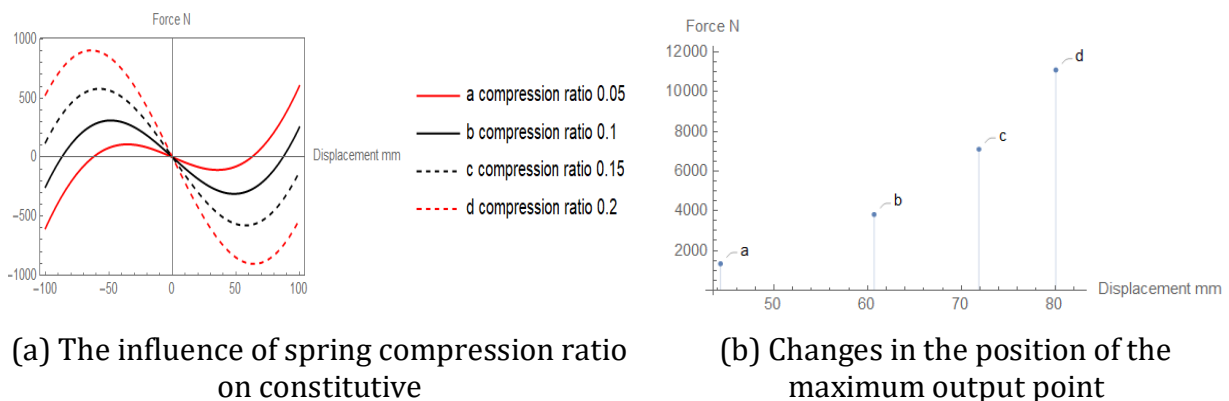


Fig. 3 Constitutive model of negative stiffness device

2.2. Analysis on the Influence of Parameters of Negative Stiffness Device.

From formula (2) and formula (3), it is not difficult to find that there are three main parameters that affect the performance of the device: spring compression ratio, spring free length and spring stiffness coefficient.

2.2.1. The Effect of Spring Compression Ratio on Negative Stiffness Devices



(a) The influence of spring compression ratio on constitutive

(b) Changes in the position of the maximum output point

Fig. 4 The influence of different compression ratios on the negative stiffness constitutive and maximum output point

The compression ratio of the spring actually indirectly controls the initial pre-pressure of the pre-compressed spring. It can be seen from Figure 4(a) that the larger the compression ratio, the greater the output of the negative stiffness device. This is because the realization of the negative stiffness force is actually the horizontal component of the spring preload, so the compression ratio cannot be too small.

At the same time, Figure 4(b) shows that the increase in compression ratio will result in the required working stroke of negative stiffness. In the application process, the working stroke is limited by the actual structure. When the displacement of the structure is too smaller than the maximum output stroke of the negative stiffness device, the negative stiffness output will be too small, which will seriously affect the practicability of the device, so the compression ratio should not be too large.

2.2.2. The Effect of Spring Compression Ratio on Negative Stiffness Devices

The compression ratio and spring length are selected as fixed values, and the spring stiffnesses are 500N/mm, 600N/mm, 700N/mm, 800N/mm, respectively. As shown in the figure below, as the stiffness increases, the maximum output of the negative stiffness device increases. As

shown in Figure 5(b), the increase in stiffness does not change the position of maximum output, so it is not difficult to conclude that by changing the stiffness of the negative stiffness device, the performance of the device can be effectively improved without changing the working stroke of the device. It is an important means to rationalize the design of negative stiffness devices.

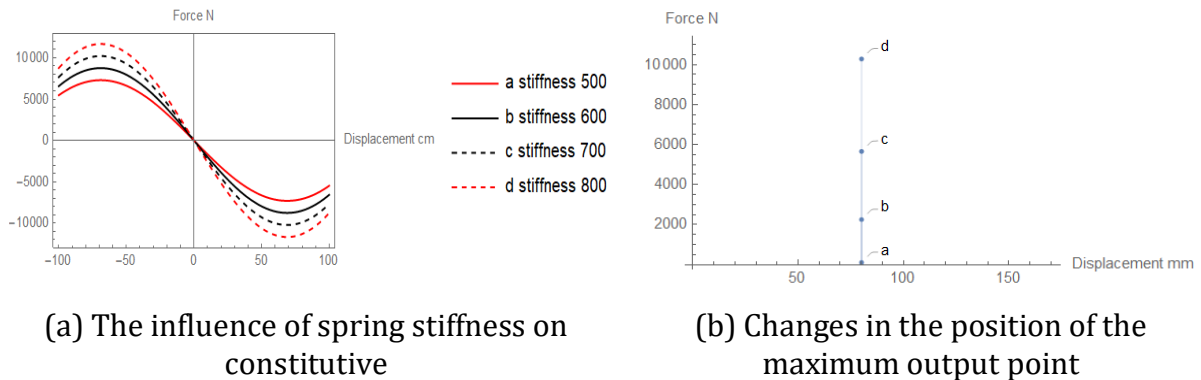


Fig. 5 The influence of different compression ratios on the negative stiffness constitutive and maximum output point

2.2.3. The Influence of the Free Length of the Spring on the Negative Stiffness Device

Under the condition that the compression ratio and stiffness of the spring are not changed, the free length of the spring is respectively taken as 200mm, 300mm, 400mm, and 500mm. The change of the free length actually changes the length of l_p . It can be found that the increase of the free length can increase the maximum output of the negative stiffness device, and at the same time lead to an increase in the position of the maximum output point. Compared with Figure 4, it is found that the increase in the maximum output point brought by the method of changing the free length to increase the output of negative stiffness is more than twice that of the method of changing the compression ratio of the spring. Therefore, the effect of changing the free length of the spring to improve the performance of the negative stiffness structure is not ideal.

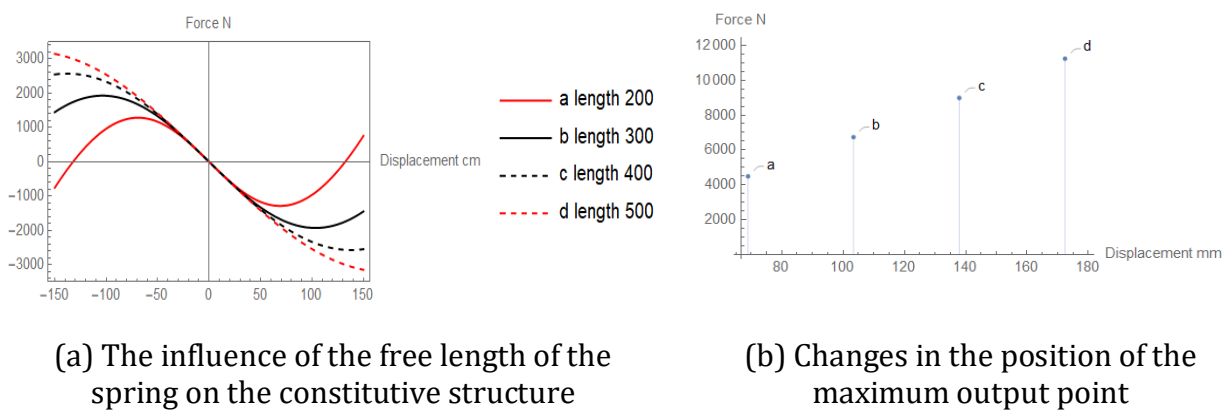


Fig. 6 The influence of the free length of the spring on the negative stiffness constitutive and the maximum output point

3. Application Analysis of Negative Stiffness Model

The negative stiffness device itself does not dissipate energy, but only reduces the structural stiffness of the building to make the internal force response of the structure smaller, while traditional energy dissipation devices such as buckling supports increase the stiffness of the

structure. Therefore, when the negative stiffness device and the buckling support are arranged in combination, the energy consumption can be increased while the building stiffness is increased by a small amount, so as to achieve the effect of reducing the seismic response.

3.1. Structural Model

A three-story concrete frame model is established, the seismic fortification intensity is 6 degrees (0.05g), the site category is I, and the designed seismic group is divided into the second group. Carry out the frame structure design of uncontrolled structure and negative stiffness structure respectively. The long side of the structure has 4 spans with a span of 6m, and the short side has 3 spans with a span of 6m. The first storey is 3.6m high and the remaining storeys are 3.3m high. The concrete strength is C30, the longitudinal reinforcement of the beam and column is HRB335, and the stirrup is HPB300. The model is shown in the figure:

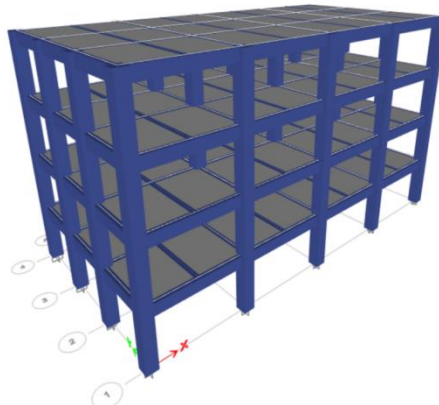


Fig. 7 Concrete frame model

For the concrete frame structure, input one-way seismic waves in the X direction and Y direction, analyze and compare the damping effect of the negative stiffness model. The beam-column section dimensions are shown in the following table.

Table 3 Sectional Dimensions of Beams and Columns

| Name | Height (mm) | Concrete | Longitudinal | Stirrup |
|----------------|-------------|----------|--------------|---------|
| Main beam | 300 | C30 | HRB335 | HPB300 |
| Secondary beam | 300 | C30 | HRB335 | HPB300 |
| column | 600 | C30 | HRB335 | HPB300 |

The adopted buckling support parameters are shown in the following table.

Table 4 Buckling Constraint Support Parameters

| Length (mm) | Area of energy-consuming section | Equivalent stiffness | Yield capacity |
|-------------|----------------------------------|----------------------|----------------|
| 6800 | 6358 | 286964 | 2000 |

3.2. Vibration Damping Plan

The Multilinear Elasticity type simulation is adopted for the negative stiffness device, and the maximum output of the device is 140KN. The anti-buckling support adopts Plastic (Wen) connection properties, and the yield index is set to 2.

Negative stiffness devices are arranged along the full height on both sides of each side of the frame structure, of which 16 are arranged in the X direction and 16 are arranged in the Y direction, a total of 32. The buckling supports are arranged on the second-story side span of the structure, of which 4 are arranged in the X direction and 4 are arranged in the Y direction, a total of 8 supports. The specific layout is shown in the figure:

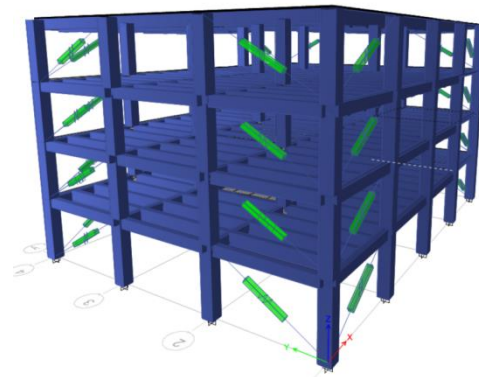
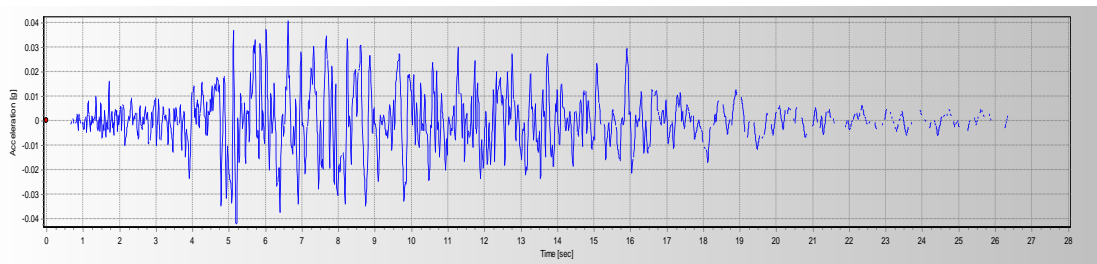


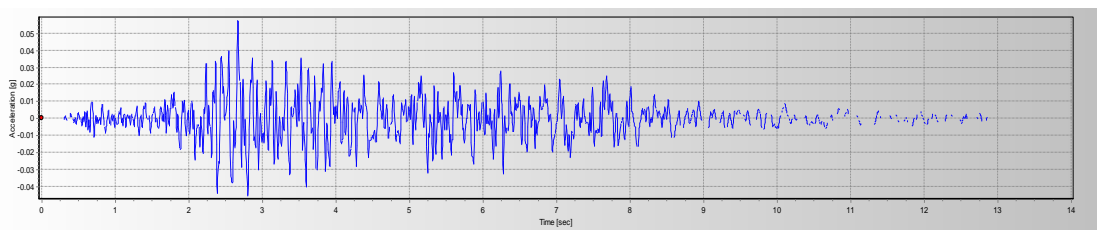
Fig. 8 Model of seismic damping layout of concrete frame

3.3. Seismic Wave Selection

The "Code for Seismic Design of Buildings" stipulates that when the time history analysis method is used, actual strong earthquake records and artificially simulated acceleration time history curves should be selected according to the type of building site and the design earthquake group. The number of actual strong earthquake records should not be less than the total number. 2/3 of. Therefore, two natural waves and one artificial wave are selected for analysis under structural fortification intensity, and the time history curve of ground motion is shown in the figure.



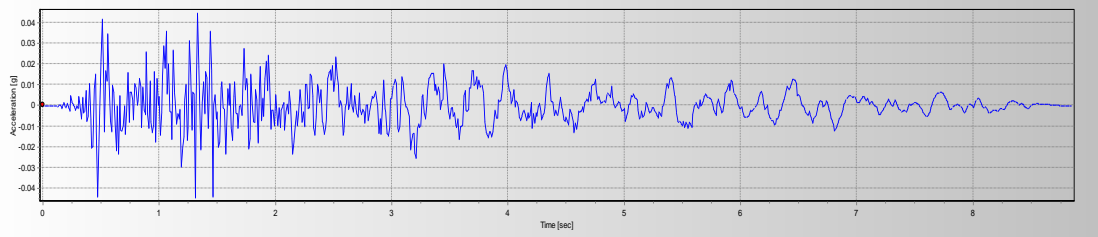
(a) LA-Hollywood Stor east-west seismic wave



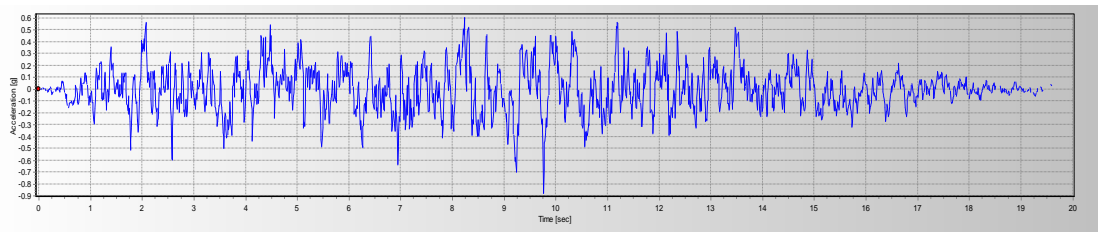
(b) LA-Hollywood Stor north-south seismic wave



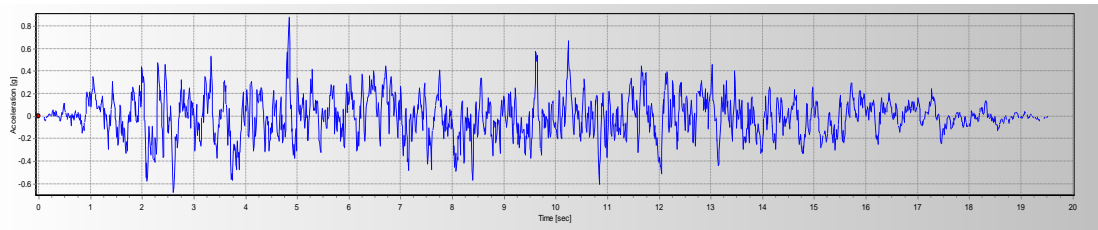
(c)Cholame-Shandon Array north-south seismic waves



(d)Cholame-Shandon Array north-south seismic wave



(e)East-west direction of artificial wave



(f)Artificial wave north-south direction

Fig. 9 Time history of earthquake acceleration

3.4. Result Analysis

According to the selected two natural seismic waves and one artificial wave, the time history analysis under frequent earthquakes is performed on the X and Y directions of the negative stiffness model and the pure frame model, respectively, and the base shear force is obtained as follows.

Table 5 Comparison of Structural base shear force under frequent earthquakes

| Seismic wave | Direction | Pure frame Base force/kN | Ratio | NS Base force/kN | Ratio |
|-------------------|-----------|--------------------------|-------|------------------|-------|
| Response spectrum | X | 2000.4 | / | 2471.9 | / |
| | Y | 1681.4 | | 2352.7 | |

| | | | | | |
|-----------------|---|--------|-------|--------|-----|
| LA - Hollywood | X | 4729.8 | 2.364 | 3404.4 | 1.4 |
| Stor | Y | 2741.6 | 1.631 | 2251.3 | 0.9 |
| Cholame - | X | 1185.4 | 0.705 | 1022.1 | 0.4 |
| Shandon Array | Y | 1435.8 | 0.854 | 1541.6 | 0.7 |
| Artificial wave | X | 2178.7 | 1.089 | 2846.5 | 1.2 |
| | Y | 1119.6 | 0.666 | 1787.8 | 0.8 |

As shown in Table 3-3, the shear force at the bottom of the structure calculated by each seismic wave is greater than 65% of the result calculated by the mode decomposition response spectrum method, and the average value of the shear force at the bottom of the structure calculated by the seismic wave is greater than the shear force value calculated by the response spectrum method. 80% of the total, so the selected two natural seismic waves and artificial waves meet the specification requirements.

Table 6 Comparison of Average interlayer displacement angles

| Seismic wave | Direction | Pure frame mean displacement | NS mean displacement | Damping rate |
|-------------------------|-----------|------------------------------|----------------------|--------------|
| Response spectrum | X | 0.00142 | 0.00107 | 24.37% |
| | Y | 0.00144 | 0.00108 | 24.66% |
| LA - Hollywood Stor | X | 0.00316 | 0.00142 | 54.97% |
| | Y | 0.00205 | 0.00098 | 52.43% |
| Cholame - Shandon Array | X | 0.00111 | 0.00057 | 48.61% |
| | Y | 0.00137 | 0.00061 | 55.84% |
| Artificial wave | X | 0.00114 | 0.00083 | 27.32% |
| | Y | 0.00166 | 0.00123 | 25.64% |

It can be seen from Table 6 that, compared with the pure frame structure, the addition of the negative stiffness device reduces the structure's maximum shelf displacement in the X direction by an average of 38.82%, and in the Y direction by an average of 39.64%. It shows that the negative stiffness can effectively reduce the displacement response of the structure under frequent earthquakes, and solve the problem of excessive inter-story displacement caused by insufficient lateral stiffness of the structure.

4. Summary

According to the theoretical analysis of the negative stiffness device proposed in this paper, it is found that an increase in the compression ratio of the pre-compression spring, an increase in the free length of the spring, and the selection of a high-strength spring will increase the negative stiffness output, but the former two will increase the working stroke of the negative stiffness device. big.

The numerical simulation of the frame structure verified that the combined arrangement of the negative stiffness-device and the anti-buckling support in the concrete frame structure can effectively control the deformation of the structure and significantly improve the seismic performance of the structure.

References

- [1] Iemura H, Pradono M H. Application of pseudo-negative stiffness control to the bench-mark cable-stayed bridge [J]. Journal of Structural Control. 2003, 10 (3-4): 187-203.
- [2] Trimboli M S, Wimmel R, Breitbach E J. Quasi-active approach to vibration isolation using magnetic springs[C].1994 North American Conference on Smart Structures and Materials. International Society for Optics and Photonics, 1994:73-83.
- [3] Platus ADL. Negative-Stiffness-Mechanism vibration isolation systems[J]. Proceedings of SPIE -The International Society for Optical Engineering, 1992,3786:44-54.
- [4] Iemura H, Pradono M H. Application of pseudo-negative stiffness control to the benchmark cable-stayed bridge[J]. Journal of Structural Control, 2003, 10(3-4):187-203.
- [5] Sun Tong. Theoretical and experimental research on negative stiffness damping system [D]. Dalian University of Technology, 2017.